

## Conductive Polymer-Coated Mesh Films with Tunable Surface Wettability for Separation of Oils and Organics from Water

Jin An, Jin-Feng Cui, Zhao-Qi Zhu, Wei-Dong Liang, Chun-Juan Pei, Han-Xue Sun, Bao-Ping Yang, An Li

Department of Chemical Engineering, College of Petrochemical Engineering, Lanzhou University of Technology, Lanzhou, People's Republic of China

Correspondence to: A. Li (E-mail: lian2010@lut.cn)

**ABSTRACT:** Here, we reported the preparation of hydrophobic mesh films by coating conductive polymers including polyaniline and polypyrrole (PPy) onto stainless steel grid through a simple electrodepositing process by combination with modification of hydrophobic materials. The hydrophobic mesh films can be used for continual separation of oils and organics from water with high selectivity. Furthermore, mesh film with reversible switching wettability from hydrophobicity to hydrophilicity can be obtained by electrodepositing of PPy in the presence of perfluorooctanesulfonate dopants at different electric potential, which makes it possible to prepare functional mesh materials with remotely controllable surface wettability for selective absorption and purification. © 2014 Wiley Periodicals, Inc. *J. Appl. Polym. Sci.* **2014**, *131*, 40759.

**KEYWORDS:** electrochemistry; films; conducting polymers; hydrophilic polymers; nanostructured polymers

Received 27 November 2013; accepted 20 March 2014

DOI: 10.1002/app.40759

### INTRODUCTION

Great efforts have been devoted to the exploiting effect materials or technology for removal of oils and organic contaminants from water owing to the global scale of severe water pollution arising from oil spills and industrial organic pollutants. The traditional approaches for cleanup of oil spills or organic contaminants typically involve the use of oil booms, barriers, and skimmers. However, obvious drawbacks of these materials rely in their hydrophilic nature with low absorption selectivity. To address these issues, superhydrophobic absorbents such as sponges,<sup>1–5</sup> activated carbon,<sup>6–9</sup> inorganic membrane,<sup>10</sup> microporous polymers,<sup>11,12</sup> macroporous gels,<sup>13</sup> and cross-linked polymer gels<sup>14–17</sup> were developed, which have been reported to possess excellent absorption selectivity, large absorption capacity, and recyclability. On the contrary, the increased interest on the fabrication of superwetting mesh films would be an additional important route to efficient oil/water separation. To date, however, only several kinds of superwetting mesh films<sup>18–28</sup> have been developed. In our previous study, a three-dimensional superwetting mesh film based on graphene assembly has also been reported to exhibit unprecedented separation and absorption performance for removal of oils (organics) from water.<sup>29</sup> Compared with those superwetting absorbents, inorganic membrane or stainless steel mesh with stable superwetting

surface properties takes great advantages of high separation selectivity, fast separation efficiency, and easy recyclability. In the most cases, however, the need of complicated fabrication techniques or high production cost or reversibility is the major obstacle that hinders their large-scale practical application. Therefore, the exploring of a simple method for preparation of efficient materials for removal of organics and oils from water should be of importance to address the environmental issues. From this point, in this work, we reported the preparation of hydrophobic and oleophilic mesh films by coating of conductive polymers such as polyaniline (PAni) and polypyrrole (PPy) onto stainless steel grid via a simple electrodepositing method. By simple assembly of such hydrophobic mesh films and a glass tube to fabricate a superoleophilic device, oils and organics could be continually separated from water with high selectivity under negative pressure. Also, this method makes it possible to prepare multifunctional mesh film materials by selecting various monomers of conductive polymers with different functionalities. For example, mesh film with reversible switching wettability was also fabricated by electrodepositing of PPy in the presence of perfluorooctanesulfonate (PFOS) dopants. We believe that such conductive polymer-coated mesh films fabricated by the simple electrodepositing method would have great potential in the applications of separation of oils and organics from water and

Additional Supporting Information may be found in the online version of this article.

© 2014 Wiley Periodicals, Inc.

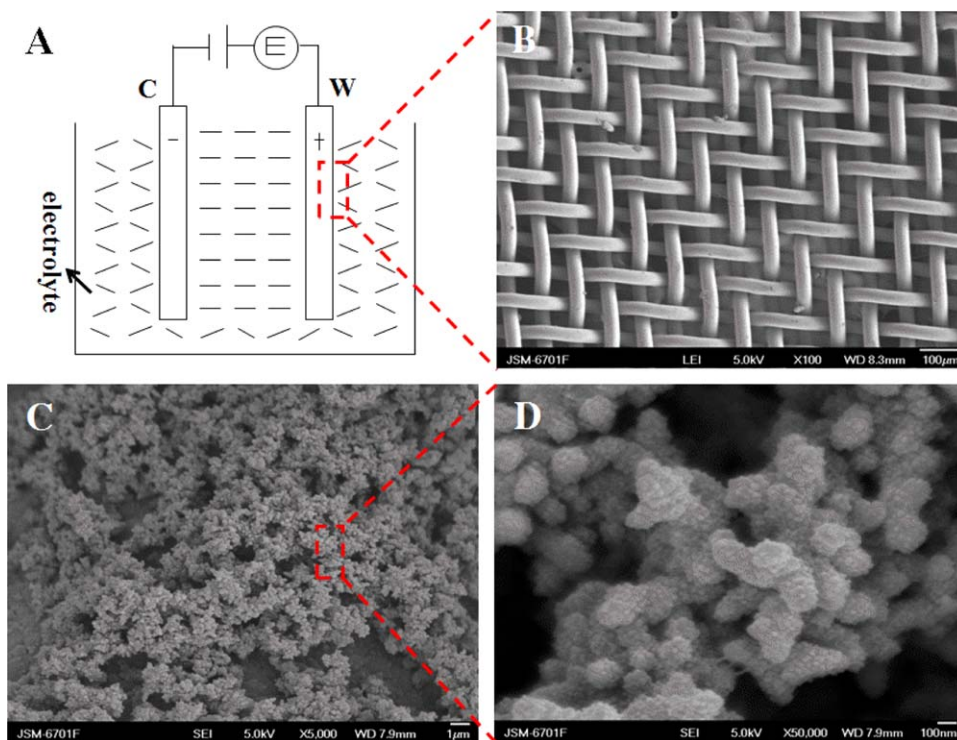


**Figure 1.** (A) A sketch map of electro-depositing device for fabrication of PAMF. (B) SEM image of pure stainless grid. (C) SEM image of the PAMF. (D) Higher-magnification SEM image of PAMF. Scale bar: (B) 100  $\mu\text{m}$ , (C) 1  $\mu\text{m}$ , (D) 100 nm. [Color figure can be viewed in the online issue, which is available at [wileyonlinelibrary.com](http://wileyonlinelibrary.com).]

is of technological significance for large-scale removal of oils and organic contaminants from water.

## EXPERIMENTAL

### Materials

Aniline (99.5%, Sigma-Aldrich) was vacuum-distilled ( $67^{\circ}\text{C}$ ) and maintained in nitrogen. Tetraethylammonium perfluorooctanesulfonate (99.8%, TEAPFOS) and pyrrole (99%) were purchased from J&K Scientific. Sulfuric acid ( $\text{H}_2\text{SO}_4$ ) and ferric chloride ( $\text{FeCl}_3$ ) were purchased from China Sinopharm Chemical Reagent and used without further purification. All the reagents are analytical grade.

**Preparation of PAni.** Stainless grid (325 mesh) with pore size of approximately  $45\ \mu\text{m}$  as a substrate was ultrasonically washed with hydrochloric acid (1M, 50 mL), distilled water, acetone, and ethanol before using. The used aqueous solution in electro-deposition process contained distilled water (100 mL), aniline (0.025 mol),  $\text{H}_2\text{SO}_4$  (0.025 mol), and  $\text{FeCl}_3$  (0.1 mg). PAni was obtained on the surface of as-treated stainless grid by electro-deposition method at 11.9 V for 15 min with two-electrode system during which the mesh grid was used as working electrode and a platinum plate was used as counter electrode [Figure 1(A)]. The resulting PAni-coated mesh film (PAMF) was washed with acetone and dried at room temperature.

**Surface Modification for PAMF.** The PAMF was dipped into a polydimethylsiloxane (PDMS) (Sylgard 184, DowCornig)/toluene solution ( $0.03\ \text{mg mL}^{-1}$ ) and dried at  $85^{\circ}\text{C}$  for 12 h. The resulting material was named as PDMS-treated PAMF.

**Preparation of PFOS-PMF.** Stainless mesh grid with pore size of approximately  $45\ \mu\text{m}$  as a working electrode was also treated ultrasonically with hydrochloric acid (1M, 50 mL), deionized water, and ethanol. The used counter electrode was a platinum sheet. Pyrrole ( $0.1\ \text{mol L}^{-1}$ ) and TEAPFOS ( $0.015\ \text{mol L}^{-1}$ ) was stirred magnetically in 100 mL acetonitrile for 30 min.  $\text{FeCl}_3$  (0.08 mmol) was used as the chemical oxidant. Oxidized PFOS-doped PPy (PFOS-PPy) was in nitrogen electro-deposited onto the stainless mesh grid with a positive potential of 5.0 V for 3 h at room temperature. The resultant oxidized PFOS-PPy-coated mesh film was defined as oxidized PFOS-PMF. Then the oxidized PFOS-PMF was washed by acetonitrile and dried at  $65^{\circ}\text{C}$  for 3 h.

**Wettability Switching Test for PFOS-PMF.** The electrolyte solution used for the wettability switching test contained  $0.015\ \text{mol L}^{-1}$  TEAPFOS in acetonitrile. The oxidized PFOS-PMF was first reduced at a negative potential of 5.0 V for 20 min with dedoping of PFOS, followed by washing with acetonitrile and drying at room temperature, in which the oxidized PFOS-PMF was converted into the reduced PFOS-PMF. Then, the reduced PFOS-PMF was re-oxidized at a positive potential of 5.0 V for 30 min, followed by washing with acetonitrile and air-dried, in which the reduced PFOS-PMF was changed into the oxidized PFOS-PMF. The contact angles (CAs) were measured after each reduction or oxidation step.

### Characterization

The morphologies of the resulting samples were examined using scanning electron microscopy (SEM) (JSM-7601F, JSM-5600LV).

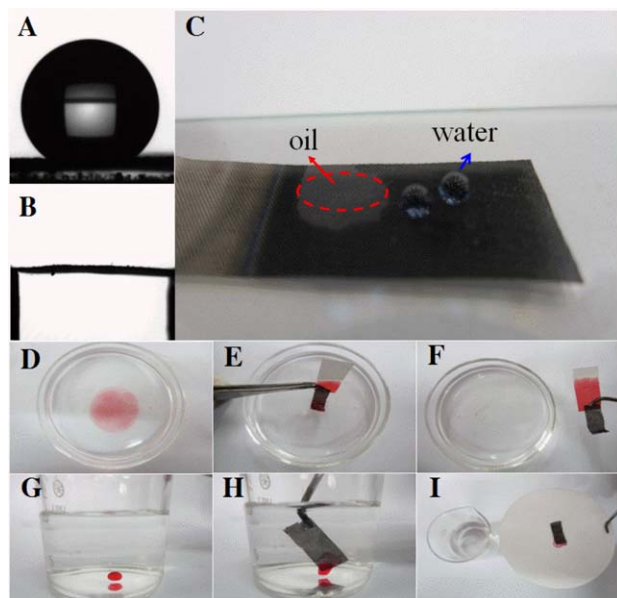


**Figure 2.** (A) Water CA measurement of PDMS-treated PAMF. (B) Diesel oil CA measurement of PDMS-treated PAMF. (C) Photograph of oil and water droplets on the surface of PDMS-treated PAMF. Photographs of PDMS-treated PAMF used for removal of octane (D–F) and chloroform (G–I) from water. [Color figure can be viewed in the online issue, which is available at [wileyonlinelibrary.com](http://wileyonlinelibrary.com).]

Solid Fourier transform infrared spectra (FT-IR) were recorded from in the range of  $4000\text{--}400\text{ cm}^{-1}$  using KBr pellet technique on a FT-Raman Module (Nicolet, USA) instrument. X-ray photoelectron spectroscopy (XPS) analysis was performed on ESCA-LAB250xi spectrometer (Thermon Scientific). The energy scale was internally calibrated by referencing to the binding energy of the C1s peak of a carbon contaminant at  $284.8\text{ eV}$ . CA measurement for samples was performed on the CA meter (DSA 100, Kruss Company, Germany). The water droplet used for Water CA measurement was  $5\text{ }\mu\text{L}$ .

## RESULTS AND DISCUSSION

In this work, PANi coating on stainless mesh grid was fabricated using electro-deposition method with an electro-depositing device, as shown in the sketch map [Figure 1(A)]. SEM was performed to evaluate the morphology of materials. As shown in Figure 1(B), the pure stainless mesh grid shows a smooth and neat surface morphology with pore size of approximately  $45\text{ }\mu\text{m}$ . After coating with PANi, the treated mesh grid exhibits a rough surface morphology composed of PANi particles with uniform diameters [Figure 1(C)]. The higher-magnification image reveals more clearly the hierarchical structures of the resulting PANi particles in which the submicrometer-sized PANi particles were covered by spines just like bulbous cactus [Figure 1(D)].

The surface wettability was evaluated by water CA measurement. Due to the hydrophilic nature of PANi, the resulting PAMF shows hydrophilic property with a water CA of  $78.5^\circ$  (Supporting Information, Figure S1). Clearly, the resulting PAMF could not be used directly for separation of organics/oils from water. So far, many kinds of mesh films with strong hydrophobicity and superoleo-

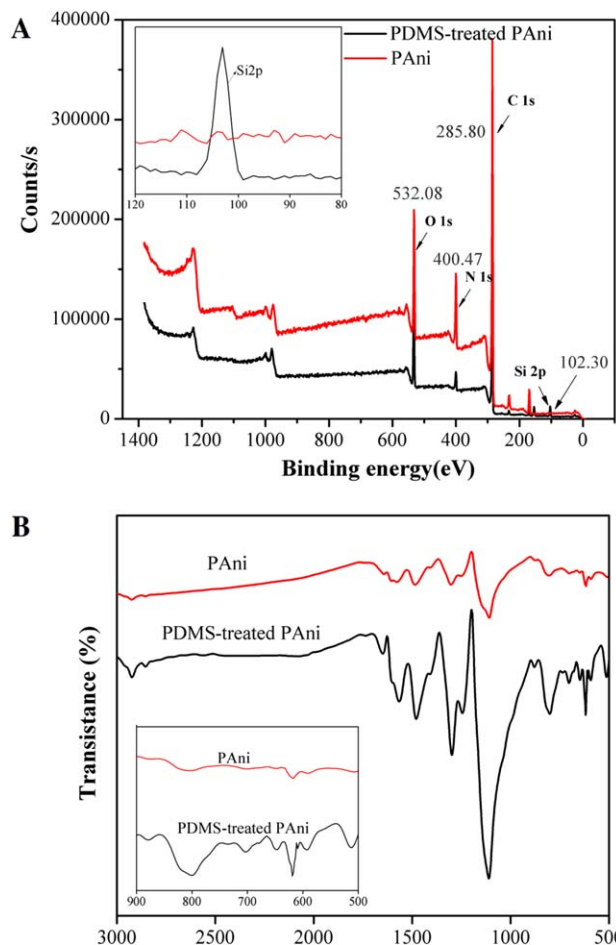


**Figure 3.** (A) XPS spectra of the synthesized PANi on the mesh grid before and after PDMS treatment; (B) FT-IR spectra of the synthesized PANi on the mesh grid before and after PDMS treatment: inset is the IR region from  $900\text{ cm}^{-1}$  to  $500\text{ cm}^{-1}$ . [Color figure can be viewed in the online issue, which is available at [wileyonlinelibrary.com](http://wileyonlinelibrary.com).]

philicity, which were achieved by surface modification with low-surface-energy materials such as polytetrafluoroethylene,<sup>30</sup> tetraethoxysilane,<sup>31</sup> and polyhedral oligomeric silsesquioxane<sup>32</sup>, have been reported and successfully used in the separation of organics/oils from water. Thus, in order to achieve high selectivity for organics/oils from water, the surface hydrophobic modification of the resulting PAMF is necessary. Inspired by these works mentioned above, we treated the PAMF with PDMS (a low-surface-energy material)<sup>33</sup> using a dip-coating method to alter its surface successfully coated on the surface of PAMF, which results in its hydrophobicity by combination with its microscopic roughness. It should be noted that the coating of PDMS on the surface of PAMF does not change its microstructure (Supporting Information Figure S2). As anticipated, the hydrophilic PAMF changes to be hydrophobic, exhibiting a water CA of  $144.8^\circ$  after treatment with PDMS, as shown in Figure 2(A). The water droplets were spherical when placed on the PDMS-treated PAMF [Figure 2(C)], indicating a hydrophobic behavior. However, a diesel oil droplet was placed on the surface and it spreaded and permeated quickly [Figure 2(C)] with an oil CA of approximately  $0^\circ$  [Figure 2(B)], indicating a superoleophilic property.



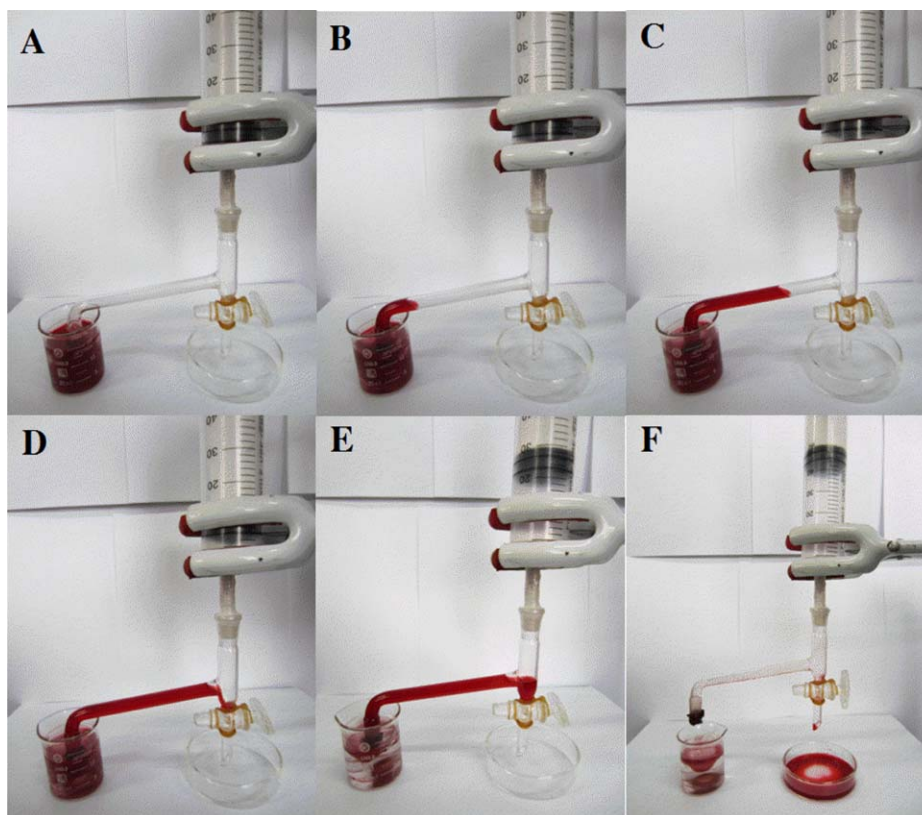


**Figure 4.** Snapshots of the separation process of octane (dyed with Red oil O) from water using PDMS-treated PAMF under negative, from A to F in sequence. [Color figure can be viewed in the online issue, which is available at [wileyonlinelibrary.com](http://wileyonlinelibrary.com).]

To further investigate the effect of surface chemical compositions on the surface wettability of PDMS-treated PAMF, XPS was performed. As seen in Figure 3(A), the peaks at 285.0 eV, 400.47 eV, and 532.08 eV are attributed to C1s, N1s, and O1s, respectively.<sup>34,35</sup> For PDMS-treated PAMF, all peaks of the as-prepared PANi on metal grid were observed. However, a new peak appeared at 102.30 eV, which is assigned to Si2p and in good accordance with previous literatures,<sup>36</sup> corresponding to 7.77 at.% silicon. That is, PDMS has been successfully coated on the surface of PAMF, which results in its hydrophobicity by combination with its microscopic roughness. It should be noted that the coating of PDMS on the surface of PAMF does not change its microstructure. The deposition of PDMS onto the PAMF was also confirmed using FT-IR spectra, as shown in Figure 3(B). The quinoid and benzenoid rings stretching bands (C=C) present at 1570  $\text{cm}^{-1}$  and 1480  $\text{cm}^{-1}$ , respectively. The characteristic peaks at 1298  $\text{cm}^{-1}$  and 1114  $\text{cm}^{-1}$  are attributed to C–N stretching and bending vibration of PANi. And the peaks observed at 810  $\text{cm}^{-1}$  and 616  $\text{cm}^{-1}$  correspond to the backbone of polyaniline.<sup>37,38</sup> For PDMS-treated PAMF, a new peak at 646  $\text{cm}^{-1}$  is observed, corresponding to the Si–O bond,<sup>39</sup> assigning to the PDMS, which suggests the successful deposition of PDMS onto the PAMF, in good agreement with the analysis of XPS.

Taking great advantages of good surface hydrophobicity and superoleophilicity, the PDMS-treated PAMF shows excellent selective absorption for organics from water. As shown in

Figure 2(D–F), when an octane droplet (dyed with Red oil O) is added into water, it could be absorbed quickly by PDMS-treated PAMF and thus can be transferred to another substrate (in this case filter paper) without absorption of water, implying a good selective absorption performance. Such observations were also observed in systems of superwetting absorbents for the selective absorption of organics or oils from water, including superwetting nanowire membranes,<sup>10</sup> carbon nanotube sponges,<sup>40</sup> and nanoporous polydivinylbenzene.<sup>17</sup> Furthermore, we found that the capture and transportation of organics (in this case chloroform) could also be performed underwater using PDMS-treated PAMF [Figure 2(G–I)]. More importantly, due to the strong affinity of PDMS-treated PAMF to organics while repelling to water, by simple assembly of the PDMS-treated PAMF and a glass tube to fabricate a superoleophilic device [Figure 4(A)], oils and organics could be continually separated from water with high selectivity under negative pressure. Figure 4 shows the separation process for octane (dyed with Red oil O) in an octane/water mixture using PDMS-treated PAMF. When the PDMS-treated PAMF was placed in the mixture solution, under negative pressure (in this case we pulled an injector to produce the negative pressure), the octane was gradually separated and collected. The separation efficiency for octane was about 85–90% in scores of experiments (SI). To our knowledge, only a few reports involved membrane materials with excellent surface wettability that were used for the separation of organic contaminants from water.<sup>10,41–44</sup> However, such dynamic absorption of

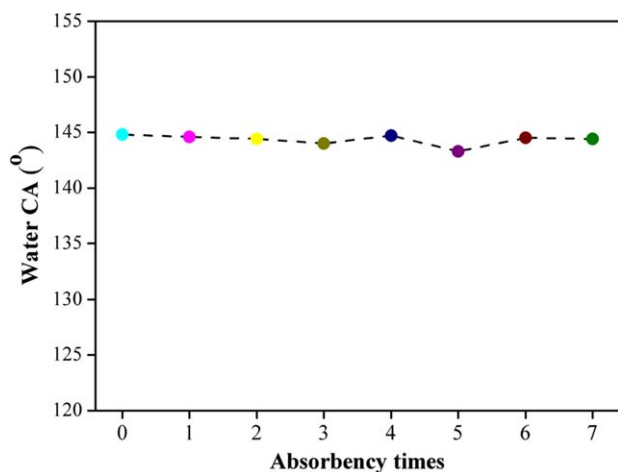


**Figure 5.** Recyclability test of PDMS-treated PAMF. PDMS-treated PAMF repetitively absorbed benzene and released its vapor under heat treatment ( $80^{\circ}\text{C}$ ) for seven cycles. [Color figure can be viewed in the online issue, which is available at [wileyonlinelibrary.com](http://wileyonlinelibrary.com).]

organics from water using PDMS-treated PAMF under negative pressure has never been reported.<sup>29,41</sup> For traditional bulk absorbent materials, the absorption efficiency mainly depends on the interaction between the absorbents and the organics<sup>45</sup> and that is an initiative and static process. In contrast, the absorption using the PDMS-treated PAMF under negative pressure is dynamic and continual, which shows advantages in the purification of organics spill or oil leakage in water on large

scale. Furthermore, compared with the recently developed superwetting inorganic films<sup>30,46</sup> or superoleophilic porous absorbents,<sup>11,17,47–49</sup> which have limitations by its bulk volume and usually show absorption capacity mostly in the range of several ten times its weight, theoretically speaking, the absorption capacity of PDMS-treated PAMF is infinite under appropriate pressure. We believe such PDMS-treated PAMF has great potentials in oil spills cleanup, especially for large areas oil leakage on sea or severe polluted water regions.

Regeneration and recyclability of materials for the removal of organics or oils from water are also important factors for the evaluation of their practical usage performance. In this case, the regeneration of the PDMS-treated PAMF can be achieved simply by heat treatment or solvent washing. Figure 5 shows the results of recyclability tests in which the PDMS-treated PAMF absorbed benzene and then was treated by heat. It can be seen that the water CA of the PDMS-treated PAMF remain nearly unchanged after seven cycles of absorption/heat test, indicating good recyclability due to the tightly wrapping of PDMS film. Importantly, this approach provides a platform capable of fabrication of hydrophobic mesh film by employment of various conductive polymers. For example, PPy-coated mesh film by electro-deposition method<sup>50</sup> was also fabricated (SI) in this study. Similarly, the resulting PPy-coated mesh film exhibits a very rough surface morphology (Supporting Information Figure S3) and a water CA of  $139.2^{\circ}$  (Supporting Information Figure S4) after treatment with PDMS. It can be observed that a number of conductive polymers such as polythiophene,<sup>51</sup> polyalkylpyrrole,<sup>52</sup> and its

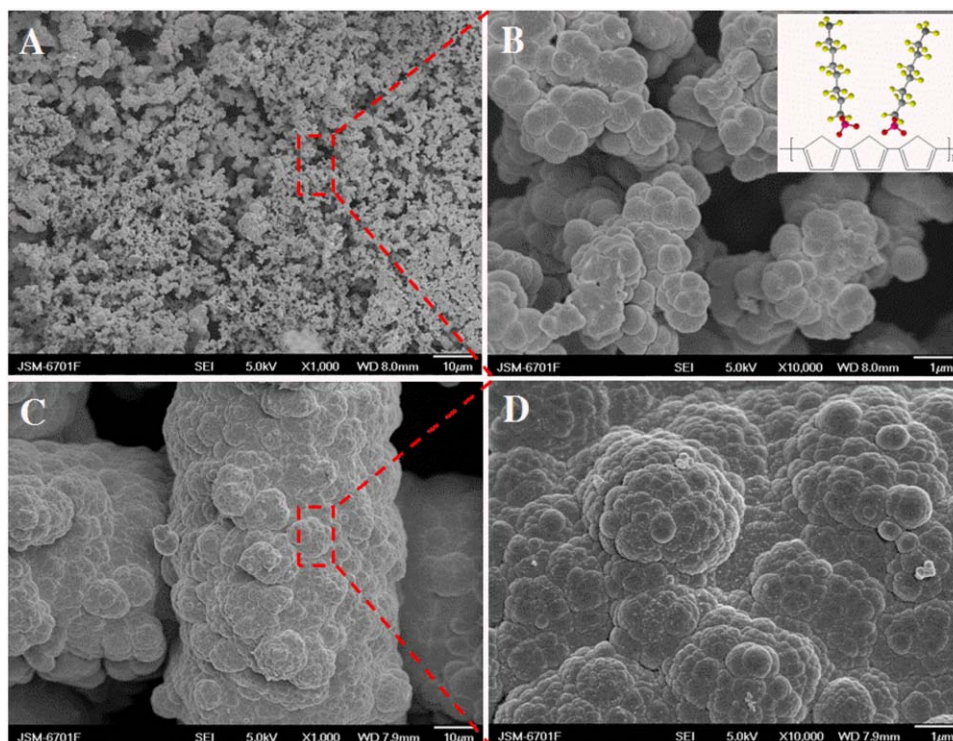


**Figure 6.** (A) SEM image of oxidized PFOS-PMF. (B) Higher-magnification SEM image of oxidized PFOS-PMF. Inset is the structure of oxidized PFOS-PMF. (C) SEM image of reduced PFOS-PMF. (D) Higher-magnification SEM image of reduced PFOS-PMF. Scale bar: (A)  $10\ \mu\text{m}$ , (B)  $1\ \mu\text{m}$ , (C)  $10\ \mu\text{m}$ , (D)  $1\ \mu\text{m}$ . [Color figure can be viewed in the online issue, which is available at [wileyonlinelibrary.com](http://wileyonlinelibrary.com).]

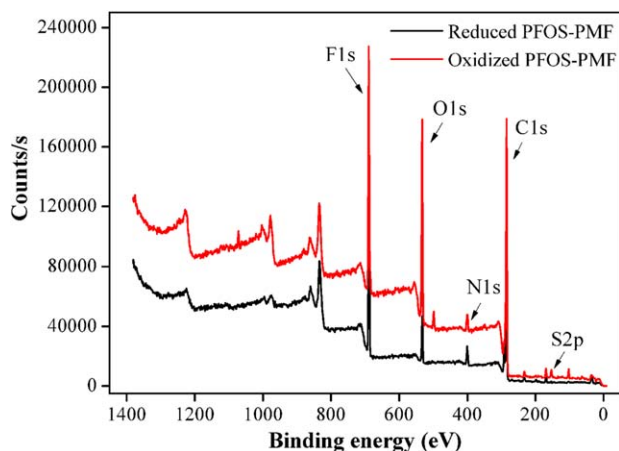


**Figure 7.** XPS spectra of oxidized and reduced PFOS-PMF. [Color figure can be viewed in the online issue, which is available at [wileyonlinelibrary.com](http://wileyonlinelibrary.com).]

derivatives<sup>53</sup> have been employed for fabrication of superhydrophobic and superoleophilic surface using electrochemical method. Thus, from this point, our study may provide a versatile method for the creation of hydrophobic mesh materials for selective absorption of oils and organics from water only by simple electro-deposition and surface modification. Furthermore, compared with those superoleophilic absorbent materials that usually were fabricated by complicated process or need multistep procedures, the fabrication of such polymer-coated mesh film using electro-deposition method and surface modification are simple, and easy to be scaled up for large-scale practical applications.

Interestingly, the multifunctional mesh films with reversible surface wettability between hydrophobicity and hydrophilicity can also be fabricated by electrodepositing special conductive polymer on the stainless mesh grid. Using the same method, the polypyrrole-coated mesh film was prepared using electrodepositing method in the presence of PFOS dopants. As shown in Figure 6(A), the oxidized PFOS-PMF shows a highly porous surface, in which the as-doped PPy particles randomly aggregated to form abundant big pores with sizes ranging from 1  $\mu\text{m}$  to 10  $\mu\text{m}$  [Figure 6(B)], resulting in a large-scale surface roughness. A water CA of 140.6° (Supporting Information Figure S5) and diesel oil CA of approximately 0° (Supporting Information Figure S6) of oxidized PFOS-PMF were measured. As a result, oils and organics (Supporting Information Figure S7) quickly pass through while water droplets remain in spherical shape, which can be used for oil/water separation. Due to the interaction between PFOS dopants and PPy film, such perfluoroalkyl short tails originated from PFOS were exposed out the surface of oxidized PFOS-PMF [Figure 6(B) inset], which existed in a strong hydrophobic and superoleophilic state of the PFOS-doped material and is well in accordance with the literatures.<sup>54–56</sup> When the electric potential of work electrode was changed from 5 V to  $-5$  V, the oxidized state of PFOS-PMF was converted into a reduced state. Quite different from the oxidized PFOS-PMF, the reduced PFOS-PMF shows a compact surface morphology [Figure 6(C,D)], which results in a hydrophilic performance with the water CA of 0° (Supporting Information Figure S8).

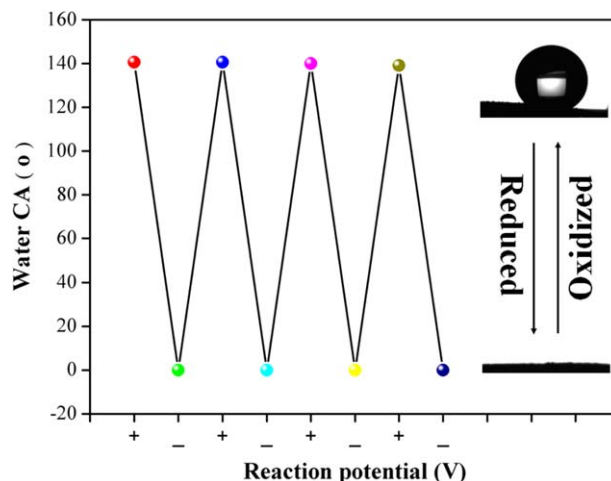


**Figure 8.** Reversibility test of the PFOS-PMF. Inset described the switchable wettability of PMF from hydrophobicity to hydrophilicity. [Color figure can be viewed in the online issue, which is available at [wileyonlinelibrary.com](http://wileyonlinelibrary.com).]

The effect of PFOS dopants on the surface wettability of PFOS-PMF was investigated on XPS. As shown in Figure 7, the peaks at 284.75 eV, 399.88 eV, 531.86 eV, 688.7 eV, and 168.57 eV are observed and attributed to C1s, N1s, O1s, F1s, and S2p, respectively.<sup>34,35</sup> Compared with the oxidized PFOS-PMF, however, the intensities of F1s and S2p peaks in the XPS spectrum of the reduced PFOS-PMF obviously decreased, which could be contributed to the fleeing of most of the PFOS dopants after reduction treatment, in accordance with the literatures.<sup>57</sup> Clearly, the loss of surface roughness in combination with a decrease of PFOS moieties [Figure 6(B) inset] on the surface of PPy lead to hydrophilic nature, which is in good agreement with previous literatures.<sup>57</sup>

The surface hydrophobicity can be regained by treating the reduced PFOS-PMF in the presence of PFOS at positive potential, suggesting a reversible surface wetting behavior between hydrophobicity and hydrophilicity. As shown in Figure 8, the water CAs of PFOS-PMF remain almost invariant even after four cycles of oxidization/reduction process, indicating good stability and reversibility due to the doping/dedoping of PFOS. It should be noted that such reversible conversion of conducting polymer films from superhydrophobic to superhydrophilic on ITO<sup>58</sup> and glass<sup>57</sup> have been reported; however, the fabrication of conductive polymer-coated mesh films with reversible switching wettability has rarely been investigated. We believe that such smart PFOS-PMF have great potential in the applications of separation of oil and organics from water. Also, the ease tailoring of wettability of PFOS-PMF only by simply adjusting the electric potential makes it possible to prepare functional mesh materials with remotely controllable surface wettability for selective absorption, purification, and so on.

## CONCLUSIONS

In summary, hydrophobic mesh films was fabricated by coating of conductive polymers including PANi and PPy onto stainless steel grid using electrodepositing method. The strong hydrophobicity and oleophilicity of the resulting mesh films should be contributed to the formation of nanostructured surface roughness of



polymers on the grid combination with low-surface-energy materials modification. The hydrophobic mesh films can be assembled for separation oils or organics from water under negative pressure, which facilitates the separation and removal of oils and organics from water on a large scale. Furthermore, by selecting various monomers of conductive polymers with different functionalities, this method also makes it possible to prepare multifunctional mesh film materials. Herein, PFOS-PMF shows a reversible switching wettability from hydrophobicity to hydrophilicity only by altering the electric potential in electrodeposition process, which makes it possible to prepare functional mesh materials with remotely controllable surface wettability for selective absorption, purification, and so on.

## ACKNOWLEDGMENTS

The authors are grateful to the National Natural Science Foundation of China (Grant No. 51263012, 51262019) and Gansu Provincial Science Fund for Distinguished Young Scholars (Grant No. 1308RJDA012).

## REFERENCES

- Choi, S. J.; Kwon, T. H.; Im, H.; Moon, D. I.; Baek, D. J.; Seol, M. L.; Duarte, J. P.; Choi, Y. K. *ACS Appl. Mater. Inter.* **2011**, *3*, 4552.
- Zhu, Q.; Chu, Y.; Wang, Z. K.; Chen, N.; Lin, L.; Liu, F. T.; Pan, Q. M. *J. Mater. Chem. A* **2013**, *1*, 5386.
- Calcagnile, P.; Fragouli, D.; Bayer, I. S.; Anyfantis, G. C.; Martiradonna, L.; Cozzoli, P. D.; Cingolani, R.; Athanassiou, A. *ACS Nano* **2012**, *6*, 5413.
- Zhu, Q.; Pan, Q. M.; Liu, F. T. *J. Phys. Chem. C* **2011**, *115*, 17464.
- Nguyen, D. D.; Tai, N. H.; Lee, S. B.; Kuo, W. S. *Energy Environ. Sci.* **2012**, *5*, 7908.
- Gui, X. C.; Wei, J. Q.; Wang, K. L.; Cao, A. Y.; Zhu, H. W.; Jia, Y.; Shu, Q. K.; Wu, D. H. *Adv. Mater.* **2010**, *22*, 617.
- Lee, C. H.; Johnson, N.; Drelich, J.; Yap, Y. K. *Carbon* **2011**, *49*, 669.
- Sun, H. X.; Li, A.; Zhu, Z. Q.; Liang, W. D.; Zhao, X. H.; La, P. Q.; Deng, W. Q. *ChemSusChem* **2013**, *6*, 1057.
- Fan, Z. L.; Qin, X. J.; Sun, H. X.; Zhu, Z. Q.; Pei, C. J.; Liang, W. D.; Bao, X. M.; An, J.; La, P. Q.; Li, A.; Deng, W. Q. *ChemPlusChem* **2013**, *78*, 1282.
- Yuan, J. K.; Liu, X. G.; Akbulut, O.; Hu, J. Q.; Suib, S. L.; Kong, J.; Stellaai, F. *Nat. nanotechnol.* **2008**, *3*, 332.
- Li, A.; Sun, H. X.; Tan, D. Z.; Fan, W. J.; Wen, S. H.; Qing, X. J.; Li, G. X.; Li, S. Y.; Deng, W. Q. *Energy Environ. Sci.* **2011**, *4*, 2062.
- Feng, L.; Song, Y. L.; Zhai, J.; Liu, B. Q.; Xu, J.; Jiang, L.; Zhu, D. B. *Angew. Chem. Int. Ed.* **2003**, *115*, 824.
- Hayase, G.; Kanamori, K.; Fukuchi, M.; Kaji, H.; Nakanishi, K. *Angew. Chem. Int. Ed.* **2013**, *52*, 1986.
- Ono, T.; Sugimoto, T.; Shinkai, S.; Sada, K. *Nat. Mater.* **2007**, *6*, 429.
- Sonmez, H. B.; Wudl, F. *Macromolecules* **2005**, *38*, 1623.
- Teblum, E. B.; Mastai, Y.; Landfester, K. *Eur. Polym. J.* **2010**, *46*, 1671.
- Zhang, Y.; Wei, S.; Liu, F.; Du, Y.; Liu, S.; Ji, Y.; Yokoi, T.; Tatsumi, T.; Xiao, F. *Nano Today* **2009**, *4*, 135.
- Zhang, J. P.; Seeger, S. *Adv. Funct. Mater.* **2011**, *21*, 4699.
- Darmanin, T.; Nicolas, M.; Guittard, F. *Phys. Chem. Chem. Phys.* **2008**, *10*, 4322.
- Wu, J.; Chen, J.; Qasim, K.; Xia, J.; Lei, W.; Wang, B. P. *J. Chem. Technol. Biotechnol.* **2012**, *87*, 427.
- Yang, J.; Zhang, Z. Z.; Xu, X. H.; Zhu, X. T.; Men, X. H.; Zhou, X. Y. *J. Mater. Chem.* **2012**, *22*, 2834.
- Crick, C. R.; Gibbins, J. A.; Parkin, I. P. *J. Mater. Chem. A* **2013**, *1*, 5943.
- Feng, L.; Zhang, Z. Y.; Mai, Z. H.; Ma, Y. M.; Liu, B. Q.; Jiang, L.; Zhu, D. B. *Angew. Chem. Int. Ed.* **2004**, *43*, 2012.
- Shang, Y. W.; Si, Y.; Raza, A.; Yang, L. P.; Mao, X.; Ding, B.; Yu, J. Y. *Nanoscale* **2012**, *4*, 7847.
- Xue, Z. X.; Wang, S. T.; Lin, L.; Chen, L.; Liu, M. J.; Feng, L.; Jiang, L. *Adv. Mater.* **2011**, *23*, 4270.
- Cao, Y. Z.; Zhang, X. Y.; Tao, L.; Li, K.; Xue, Z. X.; Feng, L.; Wei, Y. *ACS Appl. Mater. Interf.* **2013**, *5*, 4438.
- Basu, B. B. J.; Paranthaman, A. K. *Appl. Surface Sci.* **2009**, *255*, 4479.
- Razmjou, A.; Arifin, E.; Dong, G. X.; Mansouri, J.; Chen, V. *J. Membrane Sci.* **2012**, *415*, 850.
- Sun, H. X.; Li, A.; Qin, X. J.; Zhu, Z. Q.; Liang, W. D.; La, P. Q.; Deng, W. Q. *ChemSusChem* **2013**, *6*, 2377.
- Tian, D. L.; Zhang, X. F.; Wang, X.; Zhai, J.; Jiang, L. *Phys. Chem. Chem. Phys.* **2011**, *13*, 14606.
- Yang, H.; Pi, P. H.; Cai, Z. Q.; Wen, X. F.; Wang, X. B.; Cheng, J.; Yang, Z. R. *Appl. Surface Sci.* **2010**, *256*, 4095.
- Wang, H.; Xue, Y.; Ding, J.; Feng, L.; Wang, X.; Lin, T. *Angew. Chem. Int. Ed.* **2011**, *50*, 11433.
- Khorasani, M. T.; Mirzadeh, H. *J. Appl. Polym. Sci.* **2004**, *91*, 2042.
- He, Y. J.; Lu, J. H. *React. Funct. Polym.* **2007**, *67*, 476.
- Chen, S. G.; Chen, Y.; Lei, Y. H.; Yin, Y. S. *Electrochem. Commun.* **2009**, *11*, 1675.
- Hong, R.; Pan, T.; Qian, J.; Li, H. *Chem. Eng. J.* **2006**, *119*, 71.
- Huang, L. M.; Wang, Z. B.; Wang, H. T.; Cheng, X. L.; Mitra, A.; Yan, Y. S. *J. Mater. Chem.* **2002**, *12*, 388.
- Matharu, Z.; Sumana, G.; Arya, S. K.; Singh, S. P.; Gupta, V.; Malhotra, B. D. *Langmuir* **2007**, *23*, 13188.
- Zeng, Q. H.; Wang, D. Z.; Yu, A. B.; Lu, G. Q. *Nanotechnology* **2002**, *13*, 549.
- Arbatan, T.; Fang, X. Y.; Shen, W. *Chem. Eng. J.* **2011**, *166*, 787.
- Wang, C.; Tzeng, F.; Chen, H.; Chang, C. *Langmuir* **2012**, *28*, 10015.
- Kota, A. K.; Kwon, G.; Choi, W.; Mabry, J. M.; Tuteja, A. *Nat. Commun.* **2012**, *3*, 1025.
- Shi, Z.; Zhang, W.; Zhang, F.; Liu, X.; Wang, D.; Jin, J.; Jiang, L. *Adv. Mater.* **2013**, *25*, 2422.
- Zhang, W.; Shi, Z.; Zhang, F.; Liu, X.; Jin, J.; Jiang, L. *Adv. Mater.* **2013**, *25*, 2071.

45. Chen, H.; Wang, A. *J. Coll. Interf. Sci.* **2007**, *307*, 309.
46. Lee, C.; Baik, S. *Carbon* **2010**, *48*, 2192.
47. Coffinier, Y.; Janel, S.; Addad, A.; Blossey, R.; Gengembre, L.; Payen, E.; Boukherroub, R. *Langmuir* **2007**, *23*, 1608.
48. Hyun, S. K.; Dong, H. P.; Yong, B. L.; Dae-Chul, K.; Hyun-Jun, K.; Jeongyong, K.; Jinsoo, J. *Synth. Met.* **2007**, *157*, 910.
49. Bi, H. C.; Xie, X.; Yin, K. B.; Zhou, Y. L.; Wan, S.; He, L. B.; Xu, F.; Banhart, F.; Sun, L. T.; Ruoff, R. S. *Adv. Func. Mater.* **2012**, *22*, 4421.
50. Cui, X. Y.; Hetke, J. F.; Wiler, J. A.; Anderson, D. J.; Martin, D. C. *Sensor Actuat. A-Phys.* **2001**, *93*, 8.
51. Darmanin, T.; Guittard, F. *J. Am. Chem. Soc.* **2009**, *131*, 7928.
52. Mohd, K.; Jose, J. S.; Milton, A. T.; Jeison, A. F.; Vinicius, C. Z.; Andre, A. P. *J. Mater. Chem.* **2012**, *22*, 11340.
53. Hu, Y.; Kazutomo, K.; Hiroyuki, M.; Kaoru, T. *Angew. Chem. Int. Ed.* **2005**, *44*, 3453.
54. Xu, L. B.; Chen, Z. W.; Chen, W.; Mulchandani, A.; Yan, Y. S. *Macromol. Rapid Commun.* **2008**, *29*, 832.
55. Majidi, M. R.; Ashraf, S. A.; Kane-Maguire, L. A. P.; Norris, I. D.; Wallace, G. G. *Synth. Met.* **1997**, *84*, 115.
56. Lu, X. F.; Yu, Y. H.; Chen, L.; Mao, H. P.; Wang, L. F.; Zhang, W. J.; Wei, Y. *Polymer* **2005**, *46*, 5329.
57. Xu, L. B.; Chen, W.; Mulchandani, A.; Yan, Y. S. *Angew. Chem. Int. Ed.* **2005**, *44*, 6009.
58. Chang, J. H.; Hunter, I. W. *Mater. Res. Soc. Symp. Proc.* **2010**, *1228*, KK04-03.